Int J Clin Exp Med 2020;13(7):4822-4830
www.ijcem.com /ISSN:1940-5901/IJCEM0111407

Original Article

MiR-124-3p protects against acute lung injury in young rats with septic shock via regulating p38 MAPK signaling pathway

Fang Yuan[1], Runfang Hu[2], Meihong Wang[3], Jianhua Zhang[4]

[1]Department of Pediatrics, Shanghai United Family Hospital, Shanghai City, China; [2]Department of Pediatrics, Shanghai Jiao Tong University Affiliated Sixth People's Hospital, Shanghai, China; [3]Daqiao Community Health Service Center, Shanghai, China; [4]Department of Pediatric Respiratory Medicine, Xinhua Hospital Affiliated to Shanghai Jiao Tong University School of Medicine, Shanghai, China

Received March 25, 2020; Accepted April 24, 2020; Epub July 15, 2020; Published July 30, 2020

Abstract: Objective: This study aimed at exploring the protective effect of miR-124-3p on the lung of septic shock rats with acute lung injury via p38 MAPK signaling pathway. Methods: Healthy male SD rats were randomly divided into normal group (healthy rats), model group (model rats), negative control (NC) group (model rats, injected with NC vector), miR-124-3p mimic group (model rats, injected with miR-124-3p overexpression vector), miR-124-3p inhibitor group (model rats, injected with miR-124-3p silencing vector), SB203580 group (model rats, injected with p38 MAPK signaling pathway inhibitor), and miR-124-3p inhibitor + SB203580 group (model rats, combined treatment). Septic shock rat model was constructed. Results: miR-124-3p negatively regulated p38 MAPK. There were significantly reduced miR-124-3p expression, increased p-p38 MAPK/p38 MAPK expression, higher wet weight/dry weight ratio, lung permeability index (LPI), pulmonary vascular permeability (PVP), myeloperoxidase (MPO), tumor necrosis factor α (TNF-α), interleukin (IL)-6, IL-17 and IL-8 content, and lower superoxide dismutase (SOD) and glutathione (GSH) content in the rest groups as compared to normal group (all $P<0.05$). Compared with model group, there were significantly lower wet weight/dry weight ratio, LPI, PVP, MPO, TNF-α, IL-6, IL-17 and IL-8 content, and higher SOD and GSH content in miR-124-3p mimic group (all $P<0.05$), while these indexes were opposite in miR-124-3p inhibitor group. SB203580 partially repaired lung injury caused by miR-124-3p silencing, reduced MPO, TNF-α, IL-6, IL-17 and IL-8 content, and increased SOD and GSH content (all $P<0.05$). Conclusion: miR-124-3p overexpression inhibites p38 MAPK signaling pathway, thereby playing a protective effect on the lung of septic shock rats with acute lung injury.

Keywords: miR-124-3p, p38 MAPK signaling pathway, septic shock rats, acute lung injury, inflammatory factors

Introduction

Septic shock is the main cause for patients to be hospitalized in intensive care unit and even causes death [1]. The most common cause of death is multiple organ dysfunction syndrome, especially acute lung injury (ALI) and acute respiratory distress syndrome (ARDS) [2]. Septic shock usually manifests as severe hemorheological and hemodynamic changes related to organ dysfunction, including angiohypotonia, myocardial depression and hypovolemia [3]. The outcomes of septic shock-associated ALI/ARDS are worse than other kinds of ALI/ARDS [4-6]. Therefore, understanding septic shock-associated ALI/ARDS is a precondition to assess risks and optimize treatment strategies.

microRNA (miRNA) is a small non-coding RNA molecule containing about 19-24 nucleotides. It binds to the 3'-untranslated region of target mRNA to cause its degradation or to inhibit its translation so as to negatively regulate gene expression [7]. miRNA plays a vital role in fundamental biological processes, such as cell apoptosis, proliferation, differentiation, development and inflammation [8]. miR-124-3p is a subtype of miR-124 with similar biological functions to its family. miR-124-3p is significantly

reduced in Alzheimer disease and other neurodegenerative diseases, and it can improve inflammatory response in traumatic ALI [9-11]. However, it remains unclear whether miR-124-3p is involved in ALI caused by septic shock.

All eukaryotes have multiple mitogen-activated protein kinase (MAPK) pathways which control gene expression and cell physiological activities [12]. MAPK generally includes extracellular signal-regulated kinase (ERK) 1/2, p38 (α, β, γ and δ), JNK1/2/3, and big MAPK (ERK5) [13]. There have been few researches on the role of MAPK in ALI so far. p38 MAPK, one member of MAPKs superfamily, participates in important pathways regulating cell proliferation, differentiation and apoptosis [14]. MAPK signaling pathway plays a role in diseases such as cardiomegaly [15]. As a member of MAPKs, p38 MAPK can regulate gene expression level by the phosphorylation of transcription factors, thereby participating in intracellular signal transduction. The activation of p38 MAPK not only promotes the production of inflammatory factors (tumor necrosis factor α (TNF-α), interleukin (IL)-1, IL-4, IL-6, IL-8, etc.) in mononuclear macrophages, but also mediates the activation of neutrophils [16]. However, the role of p38 MAPK signaling pathway in ALI of rats with septic shock has not been illustrated fully. What's more, there is a target relationship between miR-124-3p and p38 MAPK by bioinformatics prediction, and miR-124-3p expression is down-regulated in ALI. Therefore, we speculated that miR-124-3p might target to and down-regulate p38 MAPK expression, thereby inhibiting p38 MAPK signaling pathway and suppressing ALI.

In this study, septic shock models were constructed in healthy male SD rats. Model rats were injected with miR-124-3p mimic, miR-124-3p inhibitor, p38 MAPK signaling pathway inhibitor SB203580, and miR-124-3p inhibitor + SB203580. Wet weight/dry weight ratio, lung permeability index (LPI), pulmonary vascular permeability (PVP), pathological changes, content of glutathione (GSH), superoxide dismutase (SOD) and myeloperoxidase (MPO) of the lung tissue and content of TNF-α, IL-6, IL-17 and IL-8 in bronchoalveolar lavage fluid were measured. This study aimed to explore whether miR-124-3p could target and down-regulate p38 MAPK expression to inhibit the phosphorylation of p38 MAPK signaling pathway, thereby influencing ALI in septic shock rats.

Materials and methods

Laboratory animals

The experimental protocol was approved by the Ethics Committee of Xinhua Hospital Affiliated to Shanghai Jiao Tong University School of Medicine. A total of 120 healthy young male SD rats of clean grade with the body weight of 200±235 g were enrolled in this study, of which 20 rats were taken as normal group. Model rats were divided into model group (model rats), negative control (NC) group (injected with NC vector), miR-124-3p mimic group (injected with miR-124-3p overexpression vector), miR-124-3p inhibitor group (injected with miR-124-3p silencing vector), SB203580 group (injected with p38 MAPK signaling pathway inhibitor), and miR-124-3p inhibitor + SB203580 group (combined treatment). NC, miR-124-3p mimic, miR-124-3p inhibitor and other adenovirus vector were constructed by the Tianjin Saierbio Co., Ltd., China. Rats were rapidly intraperitoneally injected with 5 μg viruses once every three days for three times. Then rats were weighed and intravenously injected with 0.5 μg/kg SB203580 (559389-1MG, Shanghai Haoran Biological Technology Co., Ltd., China). Rats, except for normal group, were intravenously injected with lipopolysaccharide (LPS) to establish septic shock model. The tube was inserted into the left femoral artery to measure mean arterial pressure (MAP) of rats. With the right femoral artery exposed, the rats were immediately injected with LPS followed by continuing observation for 1.5 h. A reduction of about 25-30% in MAP from baseline was considered as the criterion for successful construction of septic shock rat model. Rats in normal group were injected with the same amount of normal saline via the right femoral vein. The lung tissues and venous blood from the eyeball of 5 rats in each group were obtained for subsequent tests 24 h after modeling. A part of lung tissues was fixed in 10% neutral formalin solution (Solarbio) for 24 h followed by dehydration in gradient alcohol and paraffin embedding, and the rest of tissues were stored in liquid nitrogen for subsequent use.

Table 1. qRT-PCR primer sequence

Gene	Sequence
miR-124-3p	Forward: 5'-GCGAGGATCTGTGAATGCCAAA-3'
	Reverse: 5'-AGGGGCTGCTTGAGTTGTAGTA-3'
p38 MAPK	Forward: 5'-CCCGAACGATACCAGAACC-3'
	Reverse: 5'-GCGTGAATGATGGACTGAAA-3'
U6	Forward: 5'-GCTTCGGCAGCACATATACTAAAAT-3'
	Reverse: 5'-GCACTCCCGCCACAAAGATG-3'
GAPDH	Forward: 5'-GGGAAATTCAACGGCACAGT-3'
	Reverse: 5'-AGATGGTGATGGGCTTCCC-3'

Dual-luciferase reporter system

The binding site of miR-124-3p and p38 MAPK was analyzed on bioinformatics prediction website (www.targetscan.org), and the targeting relationship between them was verified by dual-luciferase reporter system. Dual-luciferase reporter gene vector of target gene p38 MAPK and the mutant in the binding site of miR-124-3p and p38 MAPK were constructed, respectively: PGL3-p38 MAPK wide type (wt) and PGL3-p38 MAPK mutant (mut). Every reporter plasmid was co-transfected respectively with miR-124-3p plasmid or NC plasmid into HEK293T cells, with rellina plasmid as internal control. After transfection for 24 h, dual-luciferase reporter assay was performed according to the instruction of dual-luciferase reporter kit (Promega). Relative luciferase activity = firefly luciferase activity/rellina luciferase activity [8].

qRT-PCR

Total RNA was extracted by Trizol (Product code 16096020, Thermo Fisher Scientific, New York, USA; Product code B1802, Harbin Haigene Testing Co., Ltd., China). TaqMan MicroRNA Assays Reverse Transcription Primer (Thermo scientific, USA) was used to reversely transcribed RNA into cDNA. SYBR®PremixExTaq™II kit (Xingzhi Biotechnology Co., Ltd., China) was used to determine fluorescence of quantitative PCR. PCR amplification solution contained 25 μL SYBR®PremixExTaq™II (2 ×), 2 μL PCR forward primer, 2 μL PCR reverse primer, l μL ROX Reference Dye (50 ×), 4 μL DNA templates, and 16 μL ddH_2O. Fluorescence quantitative PCR was performed using ABIPRISM®7300 system (Prism®7300, Shanghai Kunke Instrument Co., Ltd., China). Reaction conditions: 95°C for 10 min, 32 circles of 95°C for 15 sec and 60°C for 30 sec, and 72°C for 1 min. U6 was the internal reference of miR-124-3p, and GAPDH was for other genes. $2^{-\Delta\Delta Ct}$ showed the relative expression of target genes. Primers were shown in **Table 1**.

Western blot

Total protein was extracted using RIPA lysis buffer containing phenylmethylsulfonyl fluoride (R0010, Solarbio). Protein concentration was measured using BCA kit (Thermo, USA). Protein samples of 50 μg were loaded and electrophoresis was conducted at a constant voltage of 70 V for 3 h. Proteins were transferred to PVDF membranes (ISEQ00010, Millipore, Billerica, MA, USA) by wet method at a constant voltage of 150 mA. The membrane was sealed with 5% skimmed milk at room temperature for 2 h. Primary rabbit anti-mouse antibodies p-p38 MAPK (ab31828, 1:1,000), p38 MAPK (ab31828, 1:5,000, Abcam, UK) and GAPDH (ab22555, 1:2,000, Abcam, UK) were added onto the membrane and incubated overnight at 4°C. Horse radish peroxidase-labeled goat anti-rabbit IgG antibody (1:5,000, Beijing Zhongshan Biotechnology Co., Ltd., China) was added and incubated for 2 h. The membrane was developed according to the instruction of ECL fluorescence detection kit (Product code BB-3501, Ameshame, UK) and imaged in gel imager. Images were photographed in Bio-Rad image analysis system (BIO-RAD, USA) and analyzed by Image J software. Relative expression of the protein = gray value of target protein band/gray value of GAPDH band.

HE staining

The lung tissues were fixed in 10% neutral formalin solution for 24 h, and underwent the dehydration in gradient alcohol and the transparency with xylene (Solarbio, China). Then the tissues were embedded and cut into sections, which were then transparentized with xylene, dehydrated in gradient alcohol, and rinsed with distilled water for 1 min and stained using hematoxylin (Solarbio, China) for 3 min. Cells were differentiated using 0.5% hydrochloric acid alcohol differentiation solution (Solarbio, China) for 10 sec and rinsed with blue liquid

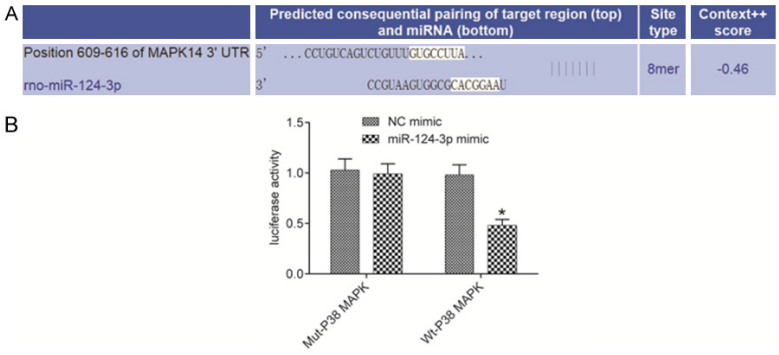

Figure 1. Targeted negative regulation of miR-124-3p to p38 MAPK. A: Sequence of 3'-UTR region in the binding site of miR-124-3p and p38 MAPK; B: Luciferase activity detection by dual-luciferase reporter assay. *P<0.05 vs. NC mimic group. NC: negative control; wt: wide type; mut: mutant.

(Solarbio, China) for 10 min, followed by staining with eosin (Solarbio, China) for 5 min. The section was dehydrated routinely, transparentized and sealed with natural gum (Solarbio, China). Sections were observed under optical microscope (XP-330, Shanghai Bingyu Optical Instrument Co., Ltd., China).

Wet weight/dry weight ratio (W/D), LPI and PVP of the lung tissue

After the left lungs of 3 rats were taken out by thoracotomy, the blood on the surface of the lung was sucked dry with filter papers to measure wet weight. After the lung was baked in a warm oven at 80°C for 48 h to achieve constant weight, dry weight was determined. W/D and water content of the lung were calculated to reflect the degree of pulmonary edema. W/D of the lung tissue = (wet weight/dry weight) × 100%. Bronchoalveolar lavage was performed in another 3 rats after thoracotomy. Cells in bronchoalveolar lavage fluid were counted and classified, and LPI (protein in bronchoalveolar lavage fluid/plasma protein) was calculated after determination of protein content. During modeling, 50 mg/kg Evans blue (Solarbio, China) was injected into the femoral vein. The lung was obtained, immersed in formamide (Solarbio, China) solution (20 mg formamide/100 g weight), and incubated at 48°C for 72 h. The samples were centrifugated to collect the supernatant. Optical density of samples at 620 nm was measured. Evans blue content was calculated according to the standard curve, and changes of PVP in each group were determined.

SOD activity, GSH and MPO content determination

The lung tissues of 125 mm^3 were added with 1 mL phosphate buffered saline to prepare tissue homogenate followed by centrifugation at 4°C and 12,000 × g for 10 min. The supernatant was collected. Protein concentration was determined using BCA detection kit (P00-11, Beyotime Biotechnology). Content of GSH, SOD and MPO in the lung tissue was measured using GSH (A003-1-2, Nanjing Jiancheng Bioengineering Institute, China), SOD (A001-3-2, Nanjing Jiancheng Bioengineering Institute, China) and MPO (K744-100, Biovision, US) activity assay kits by colorimetric method.

ELISA

After place at room temperature, blood from the eyeball was saved overnight at 4°C followed by centrifugation at 3,500 × g for 5 min. The supernatant was harvested and cryopreserved at -80°C. Levels of IL-8, IL-17, TNF-α and IL-6 were detected using the corresponding ELISA detection kits (69-30449, 69-30402, 69-25328, and 69-30490, Wuhan MSK Biotechnology Co., Ltd., China).

Statistical analysis

SPSS 21.0 statistical software was used to analyze the data. The measurement data were expressed as mean ± standard deviation. Comparison among groups was carried out by one-way analysis of variance followed by Tukey post-hoc test for pairwise comparison. The difference was statistically significant at P<0.05.

Results

miR-124-3p targeted to and negatively regulated p38 MAPK

There was a specific binding site between miR-124-3p and p38 MAPK by predicting on bioinformatics website microrna.org (http://www.microrna.org/microrna/home.do) (**Figure 1A**). According to dual-luciferase reporter assay, in

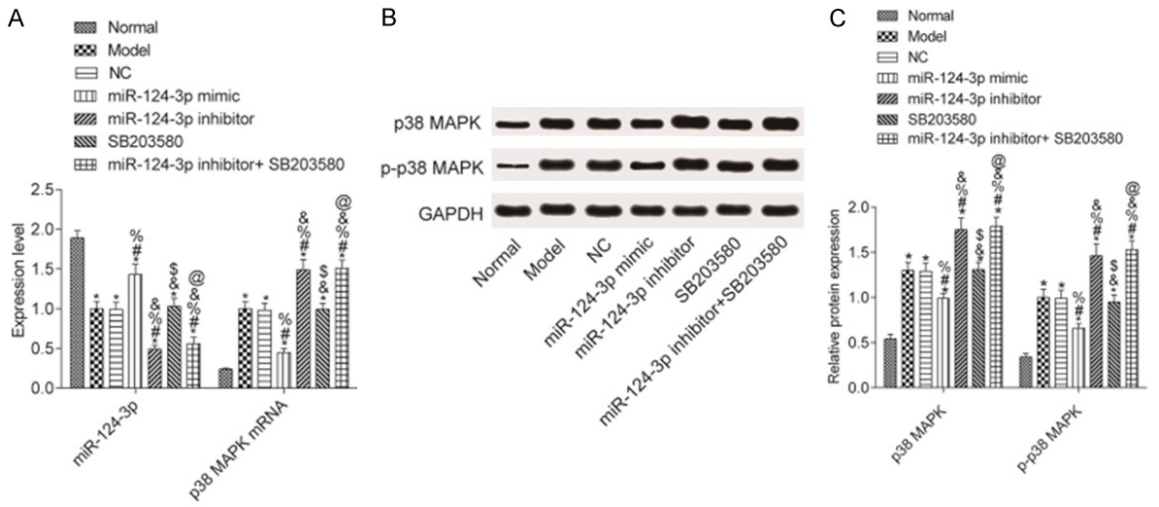

Figure 2. miR-124-3p, p38 MAPK and p-p38 MAPK expressions in the lung tissue. A: miR-124-3p and p38 MAPK mRNA expressions; B: p38 MAPK and p-p38 MAPK protein bands; C: p38 MAPK and p-p38 MAPK protein expressions. *P<0.05 vs. normal group; $^{\#}$P<0.05 vs. model group; $^{\%}$P<0.05 vs. NC group; $^{\&}$P<0.05 vs. miR-124-3p mimic group; $^{\$}$P<0.05 vs. miR-124-3p inhibitor group; $^{@}$P<0.05 vs. SB203580 group. NC: negative control.

comparison of their corresponding NC mimic co-transfected group, the group in which wt-p38 MAPK was co-transfected with miR-124-3p mimic had significantly lower luciferase activity (P<0.05), but mut-p38 MAPK group had no obvious change even co-transfected with miR-124-3p mimic (P>0.05, **Figure 1B**). The results suggested the targeted negative regulation of miR-124-3p to p38 MAPK.

Expressions of miR-124-3p and p38 MAPK in the lung tissue

There were significantly decreased miR-124-3p expression and increased p38 MAPK and p38 MAPK phosphorylation level in the rest groups compared with normal group (all P<0.05). Compared with model group, the gene expressions showed no differences in NC group, however, p38 MAPK and p-p38 MAPK expressions significantly decreased in miR-124-3p mimic group and increased in miR-124-3p inhibitor group (all P<0.05); miR-124-3p significantly increased in miR-124-3p mimic group and decreased in miR-124-3p inhibitor group and miR-124-3p inhibitor + SB203580 group (all P<0.05) (**Figure 2**).

W/D, LPI and PVP of the lung tissue

W/D, LPI and PVP were significantly higher in the rest groups than in normal group (all P<0.05). Compared with model group, W/D, LPI and PVP showed no differences in NC group and miR-124-3p inhibitor + SB203580 group, which were significantly decreased in miR-124-3p mimic group and SB203580 group and increased in miR-124-3p inhibitor group (all P<0.05). W/D, LPI and PVP were significantly lower in miR-124-3p inhibitor + SB203580 group as compared to miR-124-3p inhibitor group (all P<0.05, **Figure 3**).

Pathological changes of the lung tissue

Rats in normal group had normal bronchi and lung tissue structure, no inflammatory cells in the bronchial lumen, and normal wall thickness. There were infiltration and aggregation of eosinophilic granulocytes, lymphocytes and other inflammatory cells around the airway of rats in model group, NC group and miR-124-3p inhibitor + SB203580 group. miR-124-3p mimic group and SB203580 group showed significantly milder infiltration of inflammatory cells than model group, but the infiltration was significantly severer in miR-124-3p inhibitor group than in model group (**Figure 4**).

Content of MPO, SOD and GSH in the lung tissue

SOD and GSH content were significantly lower and MPO content was higher in the rest groups than those in normal group (all P<0.05). MPO, SOD and GSH contents showed no differences

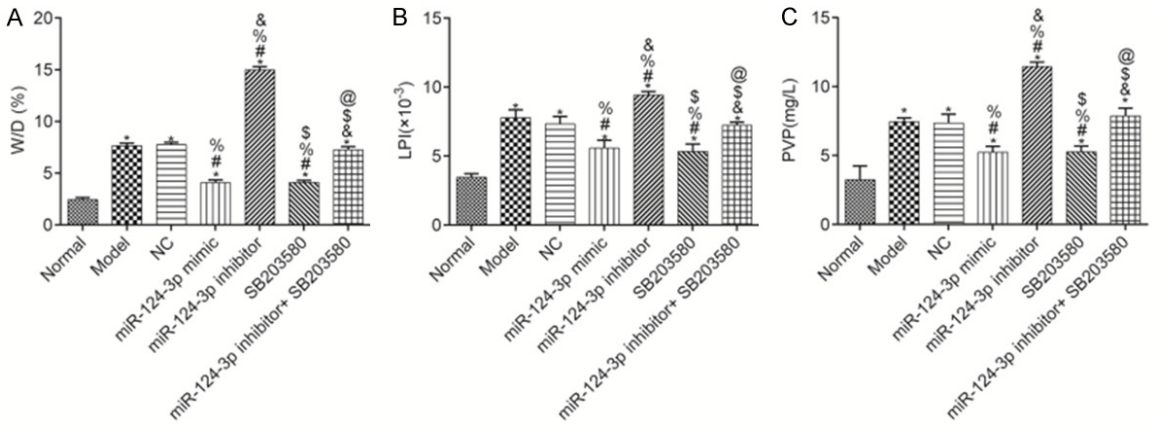

Figure 3. W/D, LPI and PVP of the lung tissue. A: Wet weight/dry weight ratio; B: Lung permeability index; C: Pulmonary vascular permeability. *P<0.05 vs. normal group; #P<0.05 vs. model group; %P<0.05 vs. NC group; &P<0.05 vs. miR-124-3p mimic group; $P<0.05 vs. miR-124-3p inhibitor group; @P<0.05 vs. SB203580 group. NC: negative control; W/D: wet weight/dry weight ratio; LPI: lung permeability index; PVP: pulmonary vascular permeability.

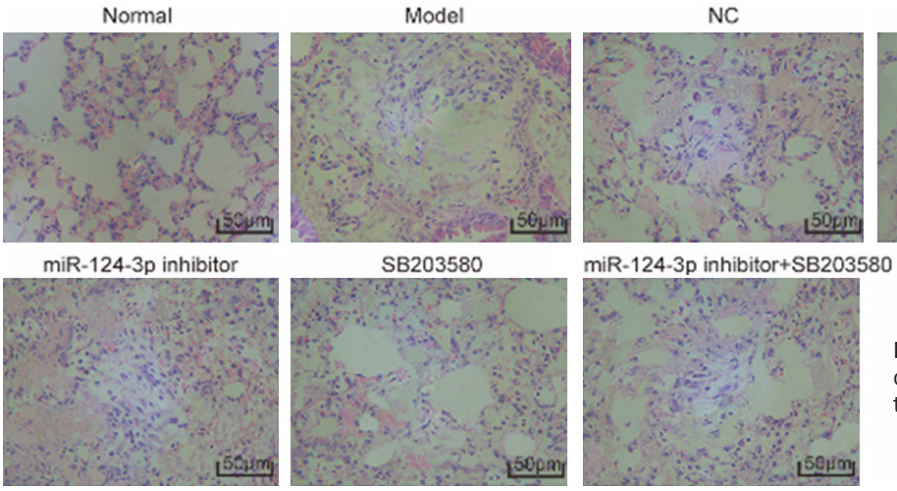

Figure 4. Pathological changes of the lung tissue (200 ×).

either between model group and NC group or miR-124-3p inhibitor + SB203580 group. When compared with model group, miR-124-3p mimic group and SB203580 group showed higher SOD and GSJ contents, as well as lower MPO content, while miR-124-3p inhibitor group showed the opposite situation (all P<0.05). SOD and GSH contents were significantly higher and MPO content was lower in miR-124-3p inhibitor + SB203580 group compared with miR-124-3p inhibitor group (all P<0.05, **Figure 5**).

Content of TNF-α, IL-6, IL-17 and IL-8 in the serum

Content of TNF-α, IL-6, IL-17 and IL-8 was significantly increased in the rest group compared with normal group (all P<0.05). Compared with model group, these cytokines showed no differences in NC group and miR-124-3p inhibitor + SB203580 group, but they were significantly lower in miR-124-3p mimic group and SB203580 group, while significantly higher in miR-124-3p inhibitor group (all P<0.05). These cytokines were significantly lower in miR-124-3p inhibitor + SB203580 group compared with miR-124-3p inhibitor group (all P<0.05, **Figure 6**).

Discussion

As far as it's known, acute lung injury (ALI) is manifested as pulmonary changes caused by various lung injuries, often leading to severe disease and even death [17]. ALI is involved in

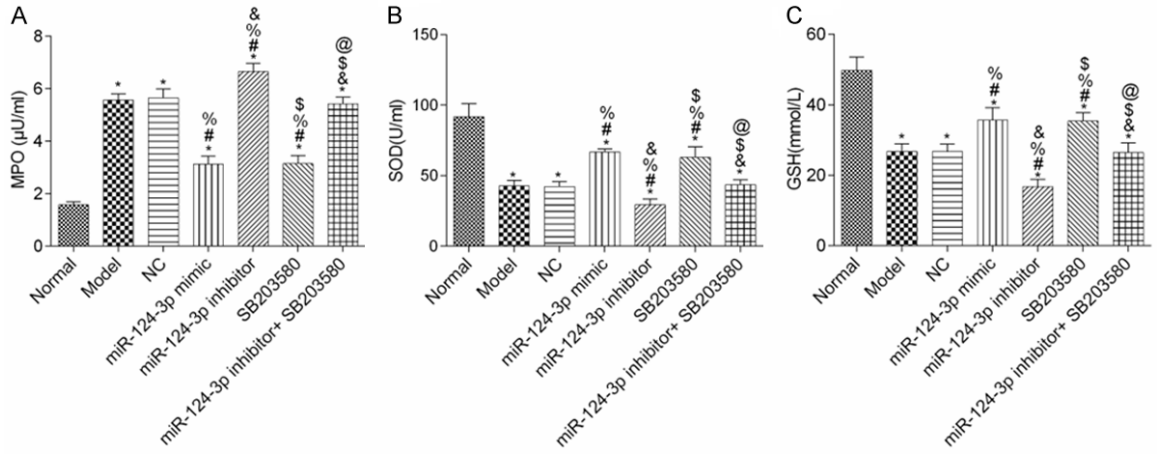

Figure 5. Content of MPO, SOD and GSH in the lung tissue. A: MPO content; B: SOD content; C: GSH content. *P<0.05 vs. normal group; #P<0.05 vs. model group; %P<0.05 vs. NC group; &P<0.05 vs. miR-124-3p mimic group; $P<0.05 vs. miR-124-3p inhibitor group; @P<0.05 vs. SB203580 group. NC: negative control; SOD: superoxide dismutase; GSH: glutathione; MPO: myeloperoxidase.

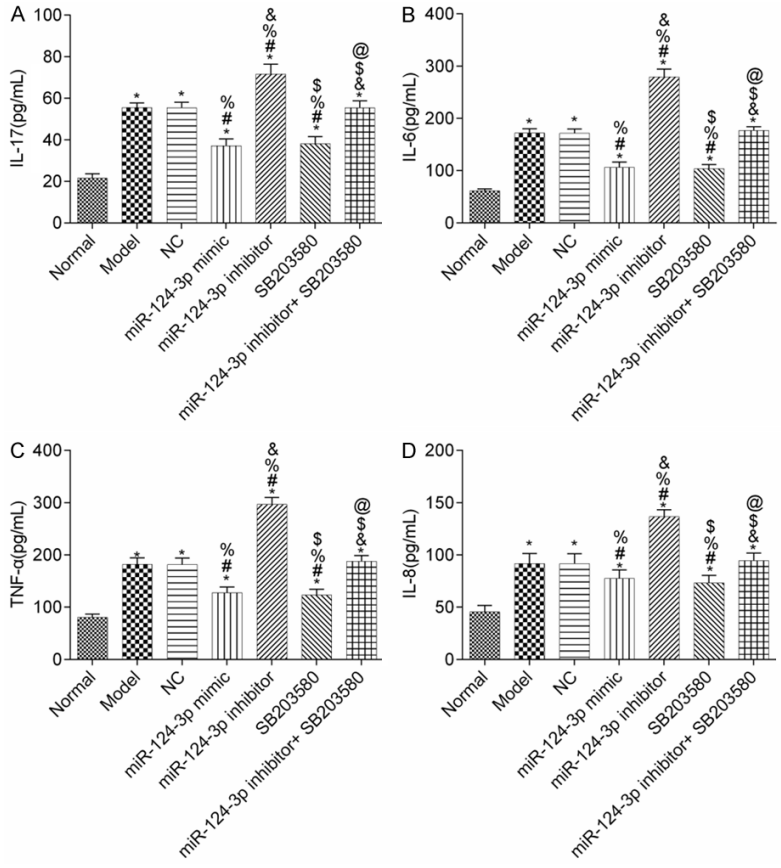

Figure 6. Content of IL-17, IL-6, TNF-α and IL-8 in the serum. A: Content of IL-17; B: Content of IL-6; C: Content of TNF-α; D: Content of IL-8. *P<0.05 vs. normal group; #P<0.05 vs. model group; %P<0.05 vs. NC group; &P<0.05 vs. miR-124-3p mimic group; $P<0.05 vs. miR-124-3p inhibitor group; @P<0.05 vs. SB203580 group. NC: negative control; TNF-α: tumor necrosis factor α; IL: interleukin.

the production of inflammatory mediators, fibrinolysis disorder, blood coagulation and oxidative damage [18]. Persistent and uncontrolled pulmonary inflammation leads to rapid alveolar damage, neutrophil infiltration and cytokine production in partial ALIs [19]. Although there are increasing researches on the mechanism and treatment of ALI, the mortality rate is still high [20]. Therefore, it is urgent to find effective treatment for septic shock patients with ALI.

The down-regulation of miR-124-3p expression is observed in multiple human diseases including atherosclerosis, Parkinson's disease and nerve injury [21-23]. p38 MAPK signaling pathway has been reported to participate in the inflammatory response of ALI/ARDS [24, 25]. The production of cytokines including IL-1β, TNF-α and IL-6 plays a key role in ALI/ARDS mainly

through p38 MPAK signal transduction pathway [26]. p38 MAPK inhibitor can inhibit the chemotaxis of neutrophils to reduce inflammatory responses, and generate superoxides to activate p38 MAPK, which leads to the increase of cytokines [27]. However, the exact mechanism of p38 MAPK signaling pathway in ALI remains to be elucidated.

In this study, down-regulation of miR-124-3p expression and up-regulation of p38 MAPK signaling pathway phosphorylation were detected in the lung tissues of septic shock/ALI rats. Consistent with previous reports, there were significantly down-regulated p38 MAPK phosphorylation level, decreased W/D, LPI and PVP, lower content of MPO, TNF-α, IL-6, IL-17 and IL-8, and higher content of SOD and GSH after p38 MAPK signaling pathway was inhibited by SB203580, indicating that the inhibition of p38 MAPK signaling pathway arrested inflammatory responses in ALI rats. To further explore the upstream regulatory mechanism of p38 MAPK, we predicted through bioinformatics website that there was a target relationship between p38 MAPK and miR-124-3p. miR-124-3p was previously attached with inhibitory effects on a variety of diseases. In this study, the negative regulation of miR-124-3p to p38 MAPK was verified by dual-luciferase reporter assay. By injecting with miR-124-3p mimic, miR-124-3p inhibitor and miR-124-3p inhibitor + SB203580 in rats, the results showed that overexpression of miR-124-3p inhibited the production of MPO, TNF-α, IL-6, IL-17 and IL-8. And compared with miR-124-3p inhibitor group, MPO, TNF-α, IL-6, IL-17 and IL-8 were significantly inhibited, and p38 MAPK phosphorylation level was down-regulated in miR-124-3p inhibitor + SB203580 group, suggesting that the inhibition of p38 MAPK phosphorylation partially repaired ALI caused by miR-124-3p silencing, and in turn inhibited the phosphorylation of p38 MAPK signaling pathway. Therefore, overexpression of miR-124-3p inhibited p38 MAPK expression, suppressed the phosphorylation of p38 MAPK signaling pathway, and then arrested ALI in septic shock/ALI rats.

This study has demonstrated that miR-124-3p modulates p38 MAPK signaling pathway by targeting p38 MAPK, thereby inhibiting ALI. This study further elucidated the pathogenesis of ALI, which established the theoretical foundation for the treatment of ALI in clinical practice. However, to confirm the above results, we need to further supplement clinical data and to identify the specific way in which p38 MAPK plays a role in p38 MAPK signaling pathway. This study also laid the foundation for exploring the association between miR-124-3p and ALI, the inhibitory effect of miR-124-3p on p38 MAPK, as well as the targeting action of miR-124-3p in ALI.

Disclosure of conflict of interest

None.

Address correspondence to: Jianhua Zhang, Department of Pediatric Respiratory Medicine, Xinhua Hospital Affiliated to Shanghai Jiao Tong University School of Medicine, No. 1665 Kongjiang Road, Yangpu District, Shanghai 200092, China. Tel: +86-021-25078999; Fax: +86-021-25078999; E-mail: zhangjianhuaxh1h@163.com

References

[1] Liu XW, Ma T, Cai Q, Wang L, Song HW and Liu Z. Elevation of serum PARK7 and IL-8 levels is associated with acute lung injury in patients with severe sepsis/septic shock. J Intensive Care Med 2019; 34: 662-668.

[2] Fujishima S, Gando S, Daizoh S, Kushimoto S, Ogura H, Mayumi T, Takuma K, Kotani J, Yamashita N, Tsuruta R, Takeyama N, Shiraishi S, Araki T, Suzuki K, Ikeda H, Miki Y, Suzuki Y, Yamaguchi Y and Aikawa N. Infection site is predictive of outcome in acute lung injury associated with severe sepsis and septic shock. Respirology 2016; 21: 898-904.

[3] Wu CT, Huang Y, Pei ZY, Xi X and Zhu GF. MicroRNA-326 aggravates acute lung injury in septic shock by mediating the NF-kappaB signaling pathway. Int J Biochem Cell Biol 2018; 101: 1-11.

[4] Jin Y, Qian J, Ju X, Bao X, Li L, Zheng S, Chen X, Xiao Z, Chen X, Zhu W, Li W, Wu W and Liang G. Osthole protects against acute lung injury by suppressing NF-kappaB-dependent inflammation. Mediators Inflamm 2018; 2018: 4934592.

[5] Wang Y, Shi C, Yang Z, Chen F and Gao L. Vitamin D deficiency and clinical outcomes related to septic shock in children with critical illness: a systematic review. Eur J Clin Nutr 2019; 73: 1095-1101.

[6] Yan XT, He XH, Wang YL, Zhang ZZ and Tang JJ. Transduced PEP-1-heme oxygenase-1 fusion protein attenuates lung injury in septic shock rats. Oxid Med Cell Longev 2018; 2018: 6403861.

[7] Huang S, Ge X, Yu J, Han Z, Yin Z, Li Y, Chen F, Wang H, Zhang J and Lei P. Increased miR-124-3p in microglial exosomes following traumatic brain injury inhibits neuronal inflammation and contributes to neurite outgrowth via their transfer into neurons. FASEB J 2018; 32: 512-528.

[8] Cui M, Wang J, Li Q, Zhang J, Jia J and Zhan X. Long non-coding RNA HOXA11-AS functions as a competing endogenous RNA to regulate ROCK1 expression by sponging miR-124-3p in osteosarcoma. Biomed Pharmacother 2017; 92: 437-444.

[9] Alvarez-Erviti L, Seow Y, Schapira AH, Rodriguez-Oroz MC, Obeso JA and Cooper JM. Influence of microRNA deregulation on chaperone-mediated autophagy and alpha-synuclein pathology in Parkinson's disease. Cell Death Dis 2013; 4: e545.

[10] Li QC, Liang Y and Su ZB. Prophylactic treatment with MSC-derived exosomes attenuates traumatic acute lung injury in rats. Am J Physiol Lung Cell Mol Physiol 2019; 316: L1107-L1117.

[11] Bittencourt-Mernak MI, Pinheiro NM, Santana FP, Guerreiro MP, Saraiva-Romanholo BM, Grecco SS, Caperuto LC, Felizardo RJ, Camara NO, Tiberio IF, Martins MA, Lago JH and Prado CM. Prophylactic and therapeutic treatment with the flavonone sakuranetin ameliorates LPS-induced acute lung injury. Am J Physiol Lung Cell Mol Physiol 2017; 312: L217-L230.

[12] Zhao L, Jiao Y, Yang AN, Cao CJ, Kong FQ, Liu XM, Yang XL and Jiang YD. The effect of miR-124 on homocysteine-induced atherosclerosis via promoter region DNA methylation in ApoE(-/-) mice. Sheng Li Xue Bao 2015; 67: 207-213.

[13] Yang J, Lin Y, Guo Z, Cheng J, Huang J, Deng L, Liao W, Chen Z, Liu Z and Su B. The essential role of MEKK3 in TNF-induced NF-kappaB activation. Nat Immunol 2001; 2: 620-624.

[14] Padda R, Wamsley-Davis A, Gustin MC, Ross R, Yu C and Sheikh-Hamad D. MEKK3-mediated signaling to p38 kinase and TonE in hypertonically stressed kidney cells. Am J Physiol Renal Physiol 2006; 291: F874-881.

[15] Feng H, Cao J, Zhang G and Wang Y. Kaempferol attenuates cardiac hypertrophy via regulation of ASK1/MAPK signaling pathway and oxidative stress. Planta Med 2017; 83: 837-845.

[16] Zhao YR, Wang D, Liu Y, Shan L and Zhou JL. The PI3K/Akt, p38 MAPK, and JAK2/STAT3 signaling pathways mediate the protection of SO2 against acute lung injury induced by limb ischemia/reperfusion in rats. J Physiol Sci 2016; 66: 229-239.

[17] Cao C, Yin C, Shou S, Wang J, Yu L, Li X and Chai Y. Ulinastatin protects against LPS-induced acute lung injury by attenuating TLR4/NF-kappaB pathway activation and reducing inflammatory mediators. Shock 2018; 50: 595-605.

[18] Chen Y, Guo L, Lang H, Hu X, Jing S, Luo M, Xu G and Zhou Z. Effect of a stellate ganglion block on acute lung injury in septic rats. Inflammation 2018; 41: 1601-1609.

[19] Guan KP, Jiang R, Xu X, Liu ZH, Liao JL, Xiong Y, Zhan H, Zeng QL and Xu J. Recombinant trichinella spiralis excretory-secretory antigen 53ku protein alleviates acute lung injury in septic mice via polarization of M2 macrophages. Zhongshan Da Xue Xue Bao Yi Xue Ban 2017; 38: 670-75.

[20] Wu KC, Huang SS, Kuo YH, Ho YL, Yang CS, Chang YS and Huang GJ. Ugonin M, a helminthostachys zeylanica constituent, prevents LPS-induced acute lung injury through TLR4-mediated MAPK and NF-kappaB signaling pathways. Molecules 2017; 22: 573.

[21] Geng L, Liu W and Chen Y. miR-124-3p attenuates MPP(+)-induced neuronal injury by targeting STAT3 in SH-SY5Y cells. Exp Biol Med (Maywood) 2017; 242: 1757-1764.

[22] de Ronde MWJ, Kok MGM, Moerland PD, Van den Bossche J, Neele AE, Halliani A, van der Made I, de Winther MPJ, Meijers JCM, Creemers EE and Pinto-Sietsma SJ. High miR-124-3p expression identifies smoking individuals susceptible to atherosclerosis. Atherosclerosis 2017; 263: 377-384.

[23] Fan X, Wang C, Shi P, Gao W, Gu J, Geng Y, Yang W, Wu N, Wang Y, Xu Y, Chen X, Zhang L, Wang K, Su B and Liu J. Platelet MEKK3 regulates arterial thrombosis and myocardial infarct expansion in mice. Blood Adv 2018; 2: 1439-1448.

[24] Xiong LL, Tan Y, Ma HY, Dai P, Qin YX, Yang RA, Xu YY, Deng Z, Zhao W, Xia QJ, Wang TH and Zhang YH. Administration of SB239063, a potent p38 MAPK inhibitor, alleviates acute lung injury induced by intestinal ischemia reperfusion in rats associated with AQP4 downregulation. Int Immunopharmacol 2016; 38: 54-60.

[25] Ma L, Zhao Y, Wang R, Chen T, Li W, Nan Y, Liu X and Jin F. 3,5,4'-Tri-O-acetylresveratrol attenuates lipopolysaccharide-induced acute respiratory distress syndrome via MAPK/SIRT1 pathway. Mediators Inflamm 2015; 2015: 143074.

[26] Bode JG, Ehlting C and Haussinger D. The macrophage response towards LPS and its control through the p38 (MAPK)-STAT3 axis. Cell Signal 2012; 24: 1185-1194.

[27] Xu X, Zhu Q, Niu F, Zhang R, Wang Y, Wang W, Sun D, Wang X and Wang A. A2BAR activation attenuates acute lung injury by inhibiting alveolar epithelial cell apoptosis both in vivo and in vitro. Am J Physiol Cell Physiol 2018; 315: C558-C570.